Minimal phrase composition revealed by intracranial recordings

Authors:

Elliot Murphy[1,2], Oscar Woolnough[1,2], Patrick S. Rollo[1,2], Zachary J. Roccaforte[1], Katrien Segaert[3,4], Peter Hagoort[4,5], Nitin Tandon[1,2,6,*]

1. Vivian L. Smith Department of Neurosurgery, McGovern Medical School, University of Texas Health Science Center at Houston, Houston, TX, USA
2. Texas Institute for Restorative Neurotechnologies, University of Texas Health Science Center at Houston, Houston, TX, USA
3. School of Psychology & Centre for Human Brain Health, University of Birmingham, Birmingham, UK
4. Max Planck Institute for Psycholinguistics, Nijmegen, The Netherlands
5. Donders Institute for Brain, Cognition and Behaviour, Nijmegen, The Netherlands
6. Memorial Hermann Hospital, Texas Medical Center, Houston, Texas, USA

*Corresponding author: Nitin Tandon (nitin.tandon@uth.tmc.edu)

Abstract

The ability to comprehend meaningful phrases is an essential component of language. Here we evaluate a minimal compositional scheme – the 'red-boat' paradigm – using intracranial recordings to map the process of semantic composition in phrase structure comprehension. 18 human participants, implanted with penetrating depth or surface subdural intracranial electrode for the evaluation of medically refractory epilepsy, were presented with auditory recordings of adjective-noun, pseudoword-noun and adjective-pseudoword phrases before being presented with a colored drawing, and were asked to judge whether the phrase matched the object presented. Significantly greater broadband gamma activity (70-150Hz) occurred in temporo-occipital junction (TOJ) and posterior middle temporal gyrus (pMTG) for pseudowords over words (300-700ms post-onset) in both first- and second-word positions. Greater inter-trial phase coherence (8-12Hz) was found for words than for pseudowords in posterior superior temporal gyrus (pSTG). Isolating phrase structure sensitivity, we identified a portion of TOJ and posterior superior temporal sulcus (pSTS) that showed increased gamma activity for phrase composition than for non-composition, while left anterior temporal lobe (ATL) showed greater low frequency (2-15Hz) activity for phrase composition, likely coordinating distributed semantic representations. Greater functional connectivity between pSTS-TOJ and pars triangularis, and between pSTS-TOJ and ATL, was also found for phrase composition. STG, ATL and pars triangularis were found to encode anticipation of composition in the beta band (15-30Hz), and alpha (8-12Hz) power increases in ATL were also linked to anticipation. These results indicate that pSTS-TOJ appears to be crucial hub in the network responsible for the retrieval and computation of minimal phrases, and that anticipation of such composition is encoded in fronto-temporal regions.

Keywords: composition, electrocorticography, semantics, posterior temporal lobe, anticipation, human, language

Introduction

How the brain integrates individual word meanings to comprehend the meaning of multi-word utterances is an issue that has vexed the cognitive neuroscience of language for decades. Although processing of single concepts is relatively well understood, how the brain computes 'complex meaning' (Hagoort, 2020) from such combinations of multiple lexical concepts is still largely a mystery. This linguistic compositional process – the combination of words into larger structures with new and complex meaning – is also referred to as "Merge" (Chomsky, 1995) or "Unification" (Hagoort, 2013).

The simplest form of studying complex meaning is by using minimal phrases. Neuroimaging studies of minimal phrasal constructions have commonly used the 'red-boat' paradigm which focuses on simple combinations of two words (Bemis and Pylkkänen, 2011, 2013; Bozic et al., 2015; Brennan and Pylkkänen, 2012; Flick and Pylkkänen, 2020; Flick et al., 2018; Pylkkänen, 2020; Westerlund and Pylkkänen, 2014; Westerlund et al., 2015), which avoids a range of confounds arising from more complex linguistic stimuli (Berwick et al., 2019). Complex meaning is only derived through compositional semantics, yielded from binary set-formation or conjunction (Chomsky et al., 2019; Pietroski, 2018). For example, "red boat" is interpreted as a boat which is red, and not a red object which hosts boat-related properties (Murphy, 2015, 2020; Pietroski, 2018), while "John ran" is interpreted as an event in which John participates, and not a type of entity that exhibits running-like features. This simple two-word semantic paradigm is ideal for use with electrophysiology, tapping into a semantic composition process that shares key features with the extraction of complex meaning from larger utterances, albeit at a different scale. Morever, a range of distinct linguistic processes conspire to interpret any given structure (Vogelzang et al., 2020).

Experimental work using the *red-boat* paradigm has most consistently implicated the left anterior temporal lobe (LATL), specifically the temporal pole, as being a crucial node in the phrase composition network at 200-250ms after the onset of the composition-marking word, e.g. the noun in adjective-noun phrases (Antonucci et al., 2008; Bemis and Pylkkänen, 2011; Lambon Ralph et al., 2012; Pobric et al., 2010; Westerlund and Pylkkänen, 2014; Wilson et al., 2014; Zhang and Pylkkänen, 2018), but also ventromedial prefrontal cortex (vmPFC) around 400ms and posterior temporal regions during a number of early processing stages (Flick and Pylkkänen, 2020; Matchin and Hickok, 2020). These studies report responses that vary in timing (between 180-350ms post-composition) and duration (50-100ms). In addition, the anatomical delineation of the 'anterior temporal lobe' is variable across these studies. Thus, both the precise locus and timing of phrase sensitivity in the human brain remains mostly unknown.

Turning to other functional loci, the left posterior temporal lobe and the angular gyrus (AG) show greater activity for sentences compared to word lists, and for phrases compared to words (Brennan et al., 2016; Matchin and Hickok, 2020). As such, posterior temporal regions are strong candidate regions for the retrieval of phrasal templates (Hagoort, 2003, 2017), with AG, LATL and frontal regions appearing to be central nodes in the composition network recruited for subsequent processing stages pertaining to further combinatorial operations at syntactic and semantic levels, and their interfaces.

In the present study, we explored which regions reliably generate cortical activity that correlates with phrasal and lexical representations. We utilized grammatical noun phrases ("red boat") and pseudoword phrases varying the position of the pseudoword ("bleeg boat", "red fulg") to isolate semantic compositional processing. Since these pseudoword phrases include phonologically viable nonwords, the differences in the second position of the phrase between these items and the grammatical noun phrases are likely a result of compositional processing. While most previous studies have presented a licensable noun ("boat"; e.g. Neufeld et al., 2016), our inclusion of an adjective-pseudoword condition ("red fulg") further isolated semantic compositionality. An early anterior negative deflection immediately preceding the critical noun in combinatorial contexts (-50–100ms) has also previously been found (Neufeld et al., 2016), which is likely an index of syntactic prediction, anticipating a noun after an adjective (Lau et al., 2006). In the present study, we further explored this issue of anticipatory composition.

Previous work in the *red-boat* paradigm has been limited by spatiotemporal resolution. Intracranial electroencephalography (iEEG) provides uniquely high spatio-temporal resolution recordings with high signal-to-noise ratio, and is also less susceptible to artifacts (e.g. muscle movements) (Arya, 2019; Flinker et al., 2011). As such, we conducted an iEEG investigation using auditory recordings of minimal adjective-noun phrases across a large patient cohort (n = 18), conducting a study of minimal phrase composition using a mixture of intracranial recordings that either penetrated grey matter or were placed directly on the cortical surface. This method permits an exploration of neural oscillations in language, with oscillations being shown to index a range of computations in the brain (Buzsáki and Watson, 2012; Hovsepyan et al., 2020; Jensen et al., 2019; Packard et al., 2020), including lexico-semantic processes (Marko et al., 2019; Prystauka and Lewis, 2019).

Results

Patients were presented with auditory recordings grouped randomly into three conditions: Adjective-Noun, Pseudoword-Noun, Adjective-Pseudoword. A subsequent colored image was

presented, and patients were tasked with responding, with a button press, to whether the image matched the phrase or not (Fig. 1A). Across the cohort, we had good coverage over lateral and medial temporal lobe, inferior parietal lobe and inferior frontal regions, with some coverage reaching into other portions of fronto-parietal and occipital regions (Fig. 1B). We saw activation in response to the auditory stimuli most prominently in superior and middle temporal regions (Fig. 1C).

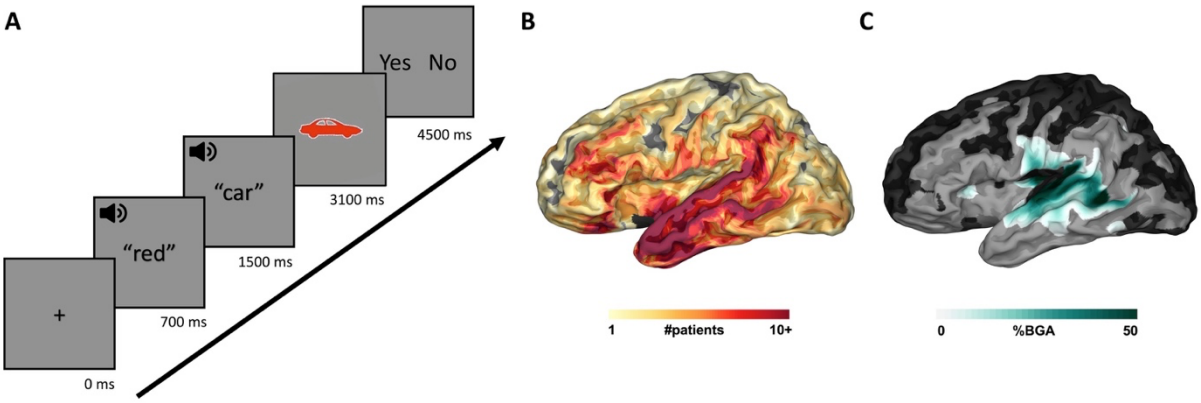

<u>Figure 1</u>: Experimental paradigm with coverage and activation maps. (A) Experimental design. Average stimuli length: adjectives (420 ± 39 ms; mean ± SD), nouns (450 ± 75 ms), pseudowords (430 ± 38 ms). (B) Group coverage map of included, left hemisphere electrodes, plotted on a semi-inflated standardised N27 surface. (C) Broadband gamma activity (BGA) increases from baseline (-500 to -100ms prior to first word) for all conditions from 100 to 400ms after onset of the first word, exhibiting sensitivity to auditory stimuli (Threshold: %BGA > 5%, t > 1.96, patient coverage ≥ 3; $p < 0.01$ corrected). Black surfaces fell below patient coverage threshold.

<u>Behavioral performance</u>

Performance in the image matching task was highly accurate 97 ± 3% (311 ± 11/320 trials) with an average response time of 1599 ± 539 ms. Only correct trials were included for analyses.

<u>Effect of lexicality</u>

Initially, to disentangle single word semantic effects from those of combinatorial semantics, we probed the difference in representation of words vs. pseudowords. To create a surface-based, population-level map of cortical activity we used surface-based mixed-effects multi-level analysis (SB-MEMA) (Conner et al., 2011; Fischl et al., 1999; Kadipasaoglu et al., 2014,

2015), a method specifically designed to account for sampling variations in iEEG and minimize effects of outliers. An SB-MEMA contrasting adjectives vs. pseudowords in word position 1 and nouns vs. pseudowords in word position 2 (Fig. 2A) revealed significantly increased broadband gamma activity (BGA; 70-150Hz) for pseudowords in posterior superior temporal gyrus (pSTG), posterior superior temporal sulcus (pSTS), temporo-occipital junction (TOJ) and pars triangularis from 300-700ms after the onset of auditory presentation, indexing additional processing effort for the unfamiliar phonology or a greater attempt to verify potential semantic content (i.e. carrying out a lexical decision). We also found greater BGA increases for pseudowords at position 2 than for position 1 around pars triangularis and surrounding frontal areas (Fig. 2C), suggesting involvement of this region in effortful lexical processing (perhaps in phonological space) and possibly semantic unification (Hagoort, 2005, 2013; Hagoort and Indefrey, 2014) or memory-related (buffer) processes.

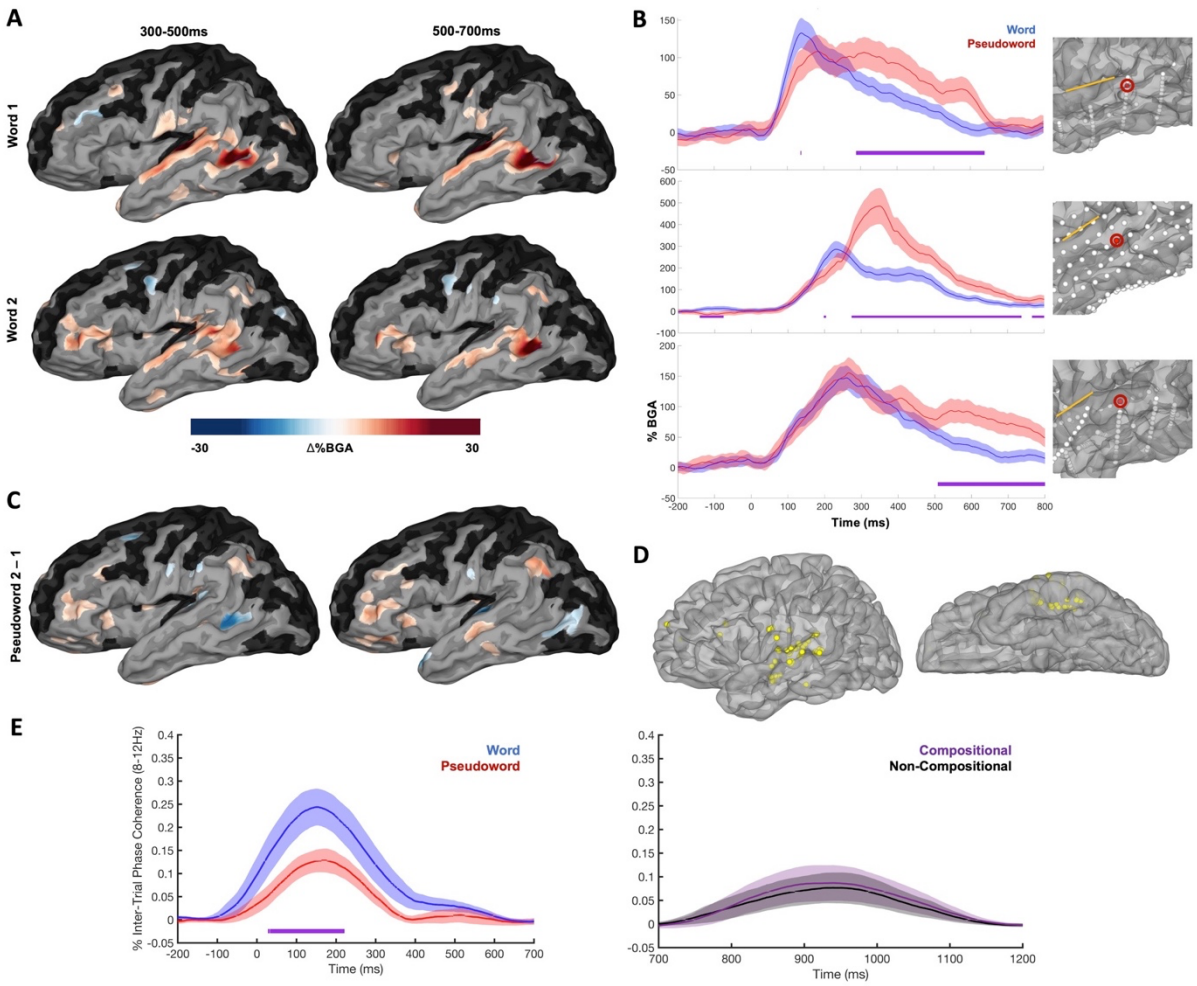

<u>Figure 2</u>: Grouped analysis for lexicality. (A) SB-MEMA comparing words vs pseudowords, with red coloration indexing greater BGA (70-150 Hz) for pseudowords and blue coloration for words (Threshold: %BGA > 5%, t > 1.96, patient coverage ≥ 3; $p < 0.01$ corrected). Top row: word position 1; bottom row: word position 2. (B) Exemplar electrodes for the words vs

pseudowords analysis (red: pseudowords; blue: words). Error bars (colored shading) set at one standard error. Sylvian fissure is marked with a yellow line for reference on each surface. (C) SB-MEMA indicating BGA increases for pseudowords at the second word position relative to pseudowords at the first word position. (D) Electrodes with significant differences in inter-trial phase coherence (ITC) for words vs pseudowords, mainly in posterior temporal cortex (9 patients). (E) ITC in alpha (8-12Hz) for all electrodes in (D) for words (blue) and pseudowords (red) on the left, and for phrase composition (purple) and non-composition (black) on the right isolated around the onset of the second word (no significant effect for composition contrast). T0 = first word onset.

Examining inter-trial phase coherence (ITC), the alpha band (8-12Hz) exclusively exhibited significantly greater ITC values for words relative to pseudowords in and around pSTG (Fig. 2D, E; Suppl. Fig. 1). No other bands or ROIs (ATL, pars triangularis, pars orbitalis, MTG, supramarginal gyrus: all FDR-corrected q-values >0.05) displayed any such effect for this or for the phrase composition contrast. Alpha phase coherence in pSTG may uniquely encode information relevant to lexical interpretation.

Phrase composition

The full combinatorial contrast (Adjective-Noun vs [Adjective-Pseudoword + Pseudoword-Noun]), revealed greater BGA for portions of pSTS-TOJ during phrase composition than non-composition during the 100-300ms SB-MEMA analysis period after noun onset (Fig. 3A). The more specific onset of this effect was around 210ms after noun onset, with peak BGA occuring around 300-350ms (Fig. 3C). This same region exhibited greater BGA for non-composition at later time windows, indicating involvement in initial phrase structure generation and evaluation (Fig. 3A, C, E). Other regions – pSTG and inferior frontal gyrus (IFG) – did not show any significant BGA differences between these conditions (Suppl. Fig. 2). While a number of discrete electrodes displayed differences in activation between 0-1000ms after the second word (Fig. 3B), only pSTS-TOJ displayed reliable effects during the early processing window. Since previous combinatorial effects in phrasal and sentential processing have also localized to anterior temporal pole, we also focused on this region (Fig. 3D, Suppl. Fig. 2). These portions of left anterior temporal lobe (temporal pole) exhibited increased low frequency (2–15Hz) activity in response to phrases from approximately 380-460ms and 700-900ms after noun presentation (Fig. 3D). This activity was unrelated to BGA (Suppl. Fig. 2), indicating that low frequency activity in ATL is an independent component of phrase structure comprehension; and given the timing, likely late-stage semantic processing. The ERPs were

dissociable from BGA across the ROIs plotted (Suppl. Fig. 2): A P300 effect for Non-Composition was found in Broca's area, likely due to greater attempted lexical access for the pseudowords, while a P600 signature was detected in temporal pole for Composition, potentially related to late-stage conceptual access.

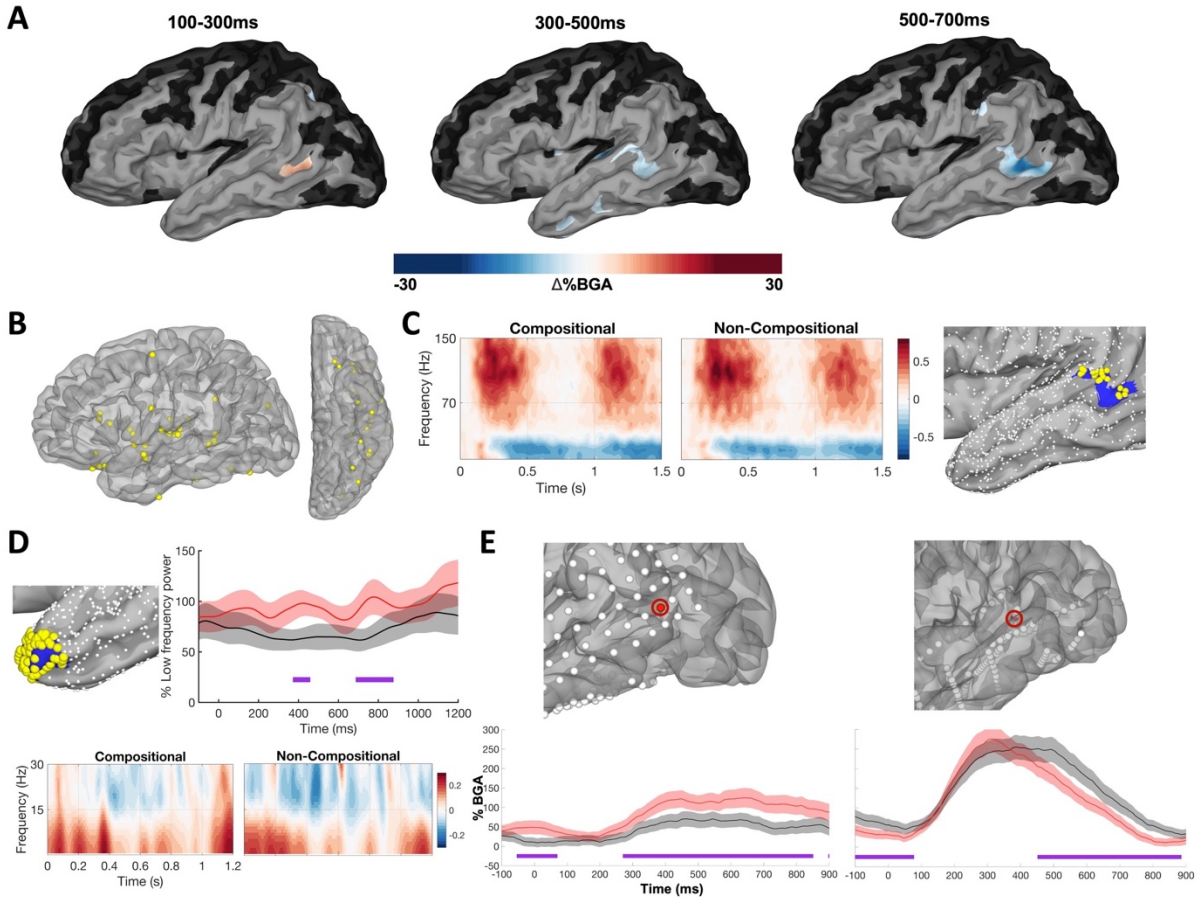

<u>Figure 3</u>: Grouped analysis for phrase composition. (A) SB-MEMAs for the phrase composition analysis for BGA. (B) Electrodes exhibiting a significant BGA contrast between Compositional and Non-Compositional trials. Out of 795 significantly active electrodes during auditory stimuli presentation, 36 (yellow) exhibited an FDR-significant contrast (one-tailed t-tests, q<0.05) between the two conditions at some point between 0-1000ms after the second word. (C) Spectrograms and electrodes in pSTS-TOJ (HCP index: TPOJ1; electrodes = 21, patients = 9). Second word onset was at 800ms. (D) Low frequency (2-15Hz) temporal pole trace with FDR-significant bars for the Compositional (red) vs Non-Compositional (black) contrast in purple (HCP index: TGd) with spectrograms below, thresholded at 10% increased activity from baseline; T0 = second word onset. (E) Exemplar electrodes with FDR-corrected (one-tailed t-tests, q<0.05) significance bars in purple plotted in native patient space. Red: Compositional. Black: Non-Compositional. Error bars set at one standard error.

Next, we further isolated regions of interest in order to examine some measure of functional connectivity during phrase composition. These were based either on the positive results of the above main analysis (pSTS-TOJ, temporal pole) or on previously-documented composition effects in the literature (pars triangularis). In addition, white matter atlas consultation reveals that the subcortical distribution of responses to semantic stimuli reflects the continuous and homogenous ventral course of functional information in the deep white matter of the temporal lobe, from TOJ, ascending to white matter underneath the posterior two-thirds of IFG (Sarubbo et al., 2020). These ventral workflow pathways subserve our regions of interest (temporal pole; TOJ; IFG). In addition, arcuate fasciculus is also classically implicated in connectivity between pSTS-TOJ and pars triangularis (Figley et al., 2017). Exploring the functional connectivity between these regions during phrase composition, we computed phase-locking values (PLV) for electrode pairs situated within pSTS-TOJ and either pars triangularis or anterior temporal lobe. We computed the generalized phase of the wideband filtered (3–50 Hz) signal. This wide band captures the dominant fluctuating components and excludes ultra-low and high frequencies to avoid spike artefacts. For instance, wideband filtering has been shown to capture the waveform of the LFP better than alpha and theta narrowband filters (Davis et al., 2020).

Of the patients with joint coverage in pSTS-TOJ and pars triangularis (n = 8, electrode pairs = 231), we found that the majority (n = 5) exhibited significantly greater PLVs for Compositional than for Non-Compositional trials during the 0-500ms period after second word onset, averaging across PLV values for each pair. Of the patients with joint coverage in pSTS-TOJ and anterior temporal lobe (temporal pole) (n = 8, electrode pairs = 274), we again found that the majority (n = 6) showed greater PLVs for the same contrast during the same time window. The timings of peak PLV differed between both interactions, with pSTS-TOJ and pars triangularis on average exhibiting the largest differences between conditions from approximately 180-500ms, and pSTS-TOJ and temporal pole exhibiting the largest differences from 250-600ms. We plot the magnitude of phase-locking values in two exemplar patients (Fig. 4).

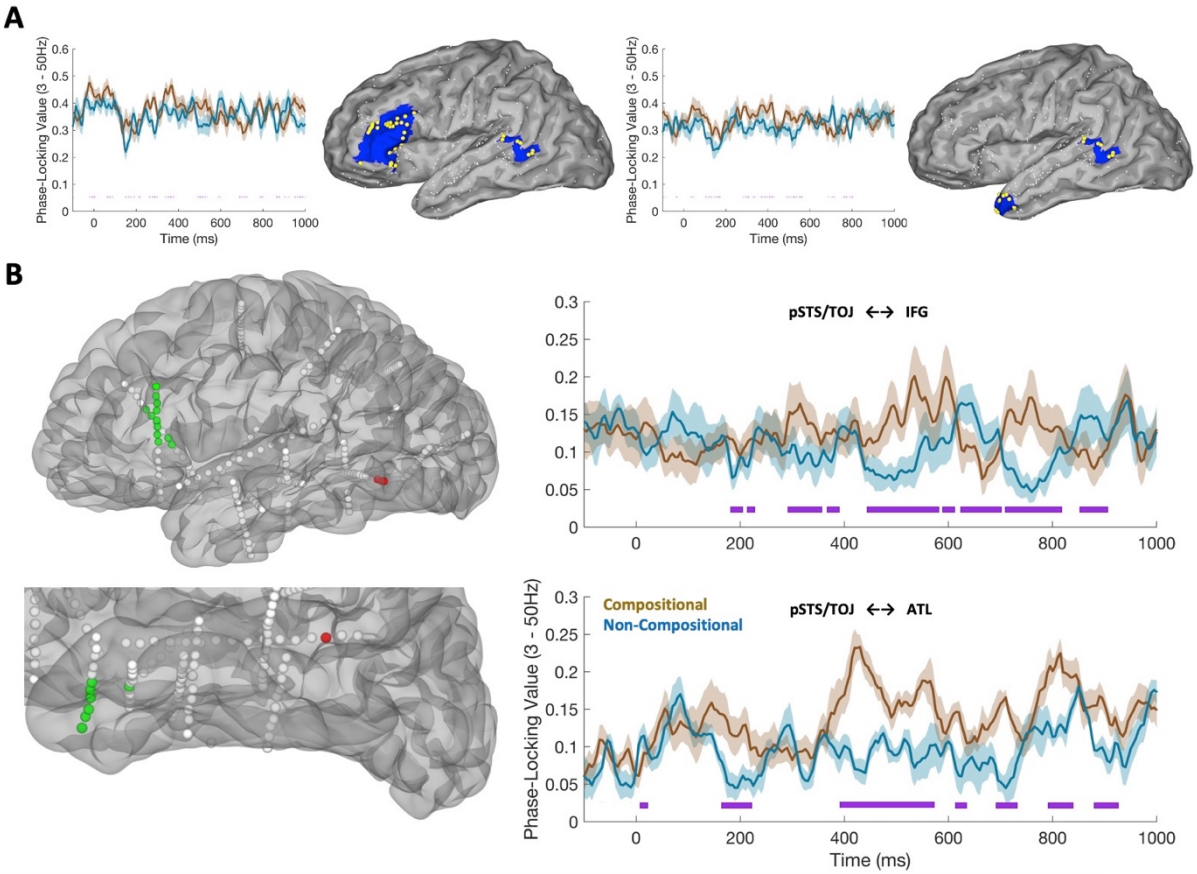

Figure 4: Phase-locking between semantic composition regions of interest. (A) Left: Average generalized phase-locking values (gPLV) for 5 patients showing greater gPLV for phrase composition relative to non-composition between pSTS-TOJ (HCP index: TPOJ1) and pars triangularis (HCP index: 45, IFSa, IFSp, 47l). Right: The same plot but for the 6 patients showing greater gPLV between pSTS-TOJ and temporal pole (HCP index: TGd). (B) Posterior temporal lobe (pSTS-TOJ) gPLVs with inferior frontal gyrus (specifically, pars triangularis) (Top) and anterior temporal lobe (specifically, temporal pole) (Bottom). Left plots show the localization in native space of electrodes significantly involved ($q < 0.05$) in inter-regional phase-locking (3 – 50 Hz). Right plots show average time courses (mean ± SEM) of phase-locking value changes from baseline in phrase composition (brown) and non-composition (blue) trials.

Compositional anticipation

We next contrasted Adjective-Noun and Pseudoword-Noun conditions at the onset of second word presentation, with only the former condition licensing any phrasal anticipation. During the anticipatory window for phrase formation (from -200ms to 0ms prior to the second word onset), the beta band (15-30Hz) exhibited an anticipatory effect (Fig. 5). This anticipatory

effect was found in LIFG, pSTG and LATL, which appear to be involved in some component of syntactic-semantic prediction generation. These results help further localize previously documented anticipatory beta increases. In addition, these anticipatory effects in beta were unrelated to modulations in BGA. For comparison, we also plot the anticipatory window in BGA for -100 to 0ms (Fig. 5B), which exhibited no relation with the lower frequency effects (compare also Fig. 5D with Fig. 5E).

We ran the same analysis for the alpha band (Fig. 5A; 8-12Hz). We found alpha increases in temporal pole, as with the beta analysis. These increases also occurred late after the presentation of the first word (600-800ms post-onset), suggesting that the effects were more likely due to anticipation rather than late-stage processing of the first word, in particular given task demands. We found only sparse, weak frontal effects. This suggests ATL involvement in a range of low frequencies during the anticipatory window, and a more isolated involvement for IFG and pSTS.

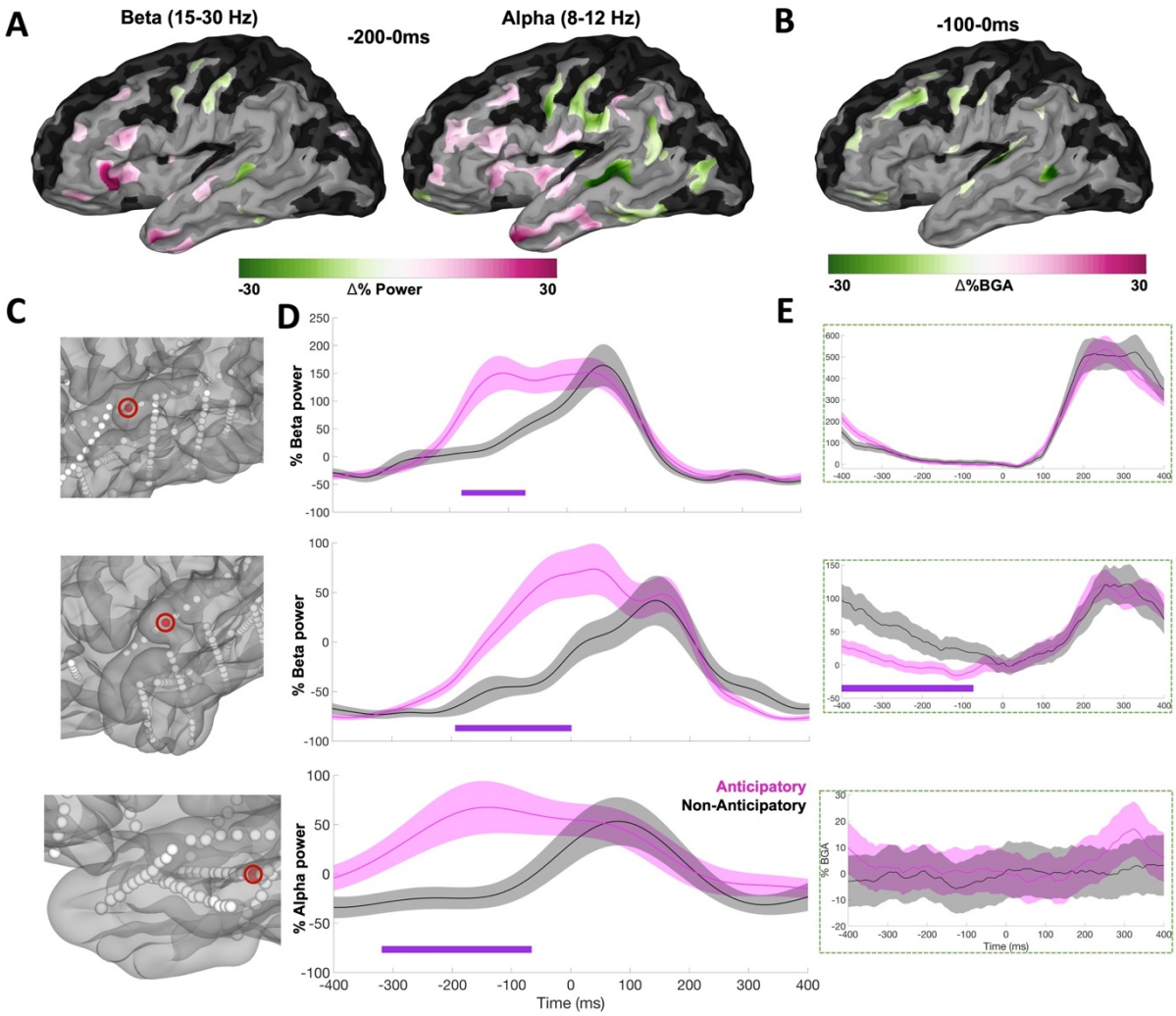

Figure 5: **Syntactic-semantic compositional anticipation.** (A) SB-MEMA for the anticipatory time window centred around second word onset (-200-0ms) for beta (left) and alpha (right). Pink: Greater beta power for composition anticipation (i.e. after having heard an Adjective at first word position). Green: Greater for no anticipation (i.e. after having heard a Pseudoword at first word position). (B) SB-MEMA for BGA for the same contrast for -100-0ms prior to second word onset. (C)-(E) Exemplar electrodes with location (C), beta or alpha power traces (pink: composition anticipation; grey: no anticipation) (D) and BGA traces in dashed green boxes (E), across three patients sorted by row.

Integration of linguistic and visual information

Following each phrase, patients were presented with a matching or non-matching visual representation of the object that had been described. Comparing the Adjective-Noun trials which contained a matching picture, or a non-matching picture, during the 250-500ms post-picture window, SB-MEMAs revealed two notable effects (Fig. 6): Anterior insula exhibited greater BGA for phrase-picture matches, while more dorsal frontal regions, centered around inferior frontal sulcus, exhibited greater BGA for phrase-picture non-matches. Thus, these regions appear to be implicated in linguistic-visual integration and monitoring, likely anchored around the semantic content denoted by both phrases and images and their successful association via some conjunction operator (i.e. [*red* ∧ *boat*], rather than a monadic adjectival or nominal representation). Interestingly, these two regions seem to straddle Broca's area, subserving distinct composition-related goals. Since activity of opercular regions can be misattributed to the insula (Woolnough et al., 2019), we ensured that these effects across patients specifically came from electrodes in insula proper, rather than operculum or Broca's area.

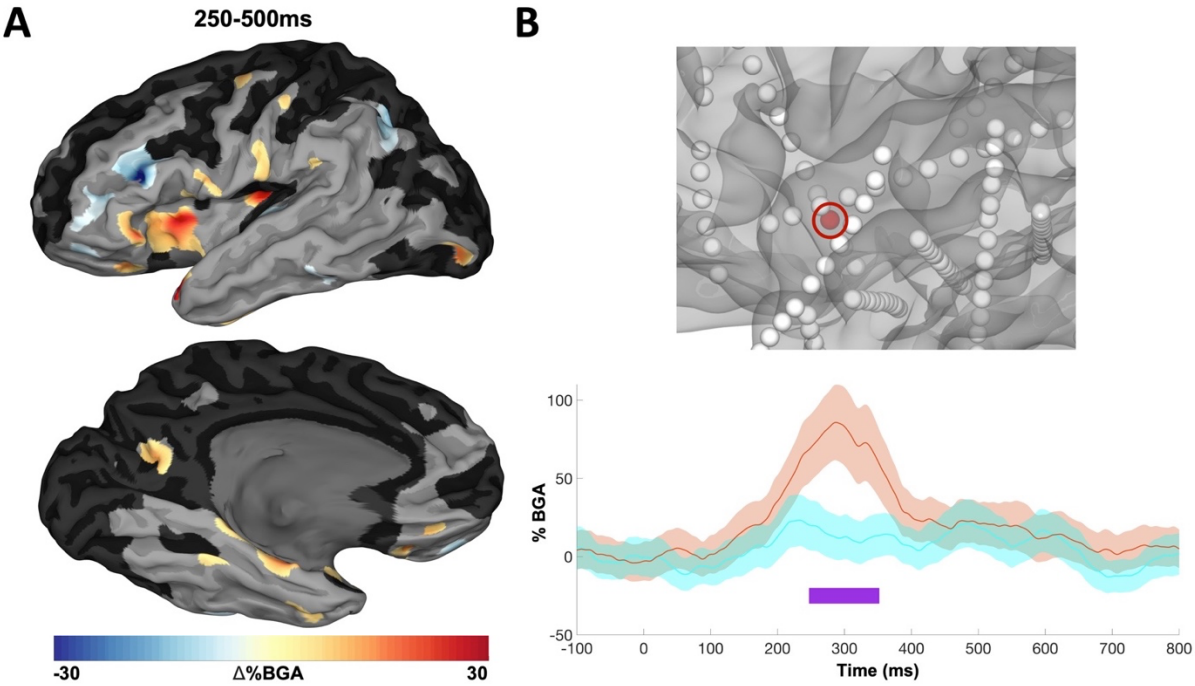

Figure 6: **Grouped analysis for linguistic-visual integration.** (A) SB-MEMA in BGA for phrase-picture match (orange) and phrase-picture contrast (turqoise) increases, 250-500ms after picture onset. (B) Exemplar insula electrode.

Discussion

We presented patients with minimal adjective-noun phrases and localised the neural correlates for combinatorial phrase structure comprehension. We found that phrase composition is indexed by two main components: Greater BGA in portions of pSTS-TOJ at an early window (around 210ms); greater low frequency power (2-15Hz) in temporal pole at 380-460ms and 700-900ms after the presentation of a phrase-licensing nominal. Greater functional connectivity for phrase composition was found between these regions (pSTS-TOJ and temporal pole) and also between pSTS-TOJ and pars triangularis, most prominently between 400-800ms after the phrase-licensing nominal. pSTS-TOJ region is initially active for phrase composition and subsequently shows greater processing effort for non-compositional stimuli, indicating its involvement in phrase-related processing. In addition, pSTS-TOJ and pSTG encode local processing of pseudowords, with pSTG likely coding speech signals into articulatory representations (Martin et al., 2019). Anterior portions of IFG exhibit greater BGA for pseudowords at the second word position, possibly indexing increased unification demands with the preceding adjective, compared to a real word (Hagoort, 2005, 2013; Hagoort and Indefrey, 2014). This effect may hence index the role of this region in the syntactic and

semantic unification of more or less expected continuations (i.e. of the adjective in first word position), in agreement with earlier results in a sentence context (Hagoort, 2004).

In addition, STG, ATL and pars triangularis index composition anticipation in beta, consistent with a predictive neural mechanism for higher-order linguistic information; findings in line with previous results (Bastiaansen and Hagoort, 2015). In ATL, alpha power exhibited increases for composition anticipation. We additionally showed that alpha phase encodes lexical information exclusively in pSTG via ITC (and not phrase-relevant information).

Lastly, anterior insula and inferior frontal sulcus subserve the integration of language input with the visual referent. Both of these regions have been argued to be the convergence zones of the ventral (anterior insula) and dorsal (IFS) attentional networks (Cazzoli et al., 2021), which may explain their recruitment in this attention-based semantic-visual task. Task-evoked pupillary dynamics have also been linked to the insula (Kucyi and Parvizi, 2020); given our picture-matching task, these dynamics may also partly underscore our findings.

Minimal composition

It is notable that one of the main candidates for phrase composition from previous research in the *red-boat* paradigm, ATL, was implicated via low frequency activity (specifically, temporal pole activity). This may indicate that temporal pole is involved in compositional processing within a noun phrase, with low frequency activity possibly coordinating broader areas of neighbouring cortex in the service of constructing a coherent semantic referent. The temporal pole involvement we found in adjective-noun binding is also compatible with known codes for object-color knowledge (Wang et al., 2020). Despite the claim that the ATL is the 'most consistent integrative node' (Pylkkänen and Brennan, 2020) in the syntax-semantics combinatorial network, and despite ATL being clearly implicated via its low frequency activity in later processing windows, the high spatiotemporal resolution of iEEG presented another candidate for composition in the form of BGA increases: pSTS-TOJ. In this connection, it has previously been shown (Flick et al., 2018) that increasing morpho-orthographic complexity in a similar minimal phrasal paradigm (using modifier-noun phrases involving head nouns that are semantically transparent compounds, e.g. "granite tombstone") does not implicate ATL in early processing windows, but seems to delay ATL activity until after intra-word morphological composition (e.g. with *tombstone*), similar to the relative timings we found. This suggests that there must be regions independent of semantic and orthographic processing that are common to all forms of (early) phrasal composition. Our findings suggest that pSTS-TOJ might be one such region, although since we only presented auditory stimuli we cannot make any stronger claims here. Comparing the discovered composition effect in BGA (Fig. 3A) with the auditory stimuli activation map (Fig. 1C) suggests a clear overlap between sites of initial sensitivity to

auditory stimuli (in posterior temporal sites in Fig. 1C) and composition-sensitive sites (in pSTS-TOJ in Fig. 3A), which may indicate that we are tapping into a modality-specific compositional process. On the other hand, while there is indeed overlap between these sites, there is also a portion of posterior TOJ which seems uniquely active for composition but which is not prominently sensitive to audition, which may point to the involvement of a more modality-independent compositional process. Since MEG cannot detect high frequency activity deep in sulci (Irimia et al., 2012), our iEEG investigation was uniquely able to detect this activity. Moreover, our finding of only an average of 10-20% in BGA increases in pSTS-TOJ for composition relative to non-composition speaks to the apparent subtlety in local processing differences needed for higher cognitive functions like compositionality.

The timing of composition effects we found – from early in pSTS-TOJ (for BGA) to later in temporal pole (for low frequencies) – appears to mirror previous findings (Flick et al., 2018). Our 100-300ms window showed greater BGA increases for phrase composition in pSTS-TOJ, and inspection of individual traces and summated activity (Fig. 3C, E) suggests onset around 210ms and diminishing around 350ms, after which the majority of responses were greater for non-compositional trails. It is possible that the composition-specific computations initiated earlier than this, and that it was only during these time windows that condition differences arose. It is also possible that the two low frequency responses we found to composition in ATL at 380-460ms and 700-900ms post-noun onset are responses to post-syntactic (pSTS-TOJ) processing, leading to conceptual integration. The timing of these late wrap-up effects might be due to the slow nature of these frequencies and could also be due to some form of traveling oscillatory component (Muller et al., 2018) from posterior temporal areas, or to the nature of the semantic computations involved.

Our findings are in line with recent models implicating these posterior portions of temporal lobe in phrase structure building (Flick and Pylkkänen, 2020; Matchin and Hickok, 2020; Murphy, 2018, 2020), a recent meta-analysis of sign language implicating TOJ and pMTG/pSTS in comprehension (Trettenbrein et al., 2020), and the finding that cross-linguistic (French and Chinese) reading competence is linked to pSTS (Feng et al., 2020), contributing to the neural localization of a modality-independent compositional operator (Chomsky et al., 2019; Pietroski, 2018), an essential component of language. In particular, evidence from neuroimaging and lesion-deficit mapping indicates a role for pMTG in syntactic comprehension and production (Matchin and Hickok, 2020), while pSTS has been implicated via iEEG in hierarchical syntactic computations (Nelson et al., 2017). Posterior temporal regions also provide the strongest and most reliable syntax-specific effects when interpreting lists of nouns embedded within sentences compared to such noun lists in isolation (Law and Pylkkänen, 2021). More broadly, pMTG is robustly associated with basic phrase

comprehension deficits across a large number of studies. Data from brain stimulation implicate postero-middle temporal areas in syntactic processing (Duffau et al., 2014), and another recent *red-boat* study in fMRI implicated a broad portion of pMTG in meaningful phrase composition (Graessner et al., 2021). Impairments in grammaticality judgments have primarily been linked to posterior temporal lobe damage (Wilson and Saygin, 2004). Lastly, widespread monotonic fronto-temporal language network gamma power increases over the course of sentence reading have been discovered previously in iEEG (Fedorenko et al., 2016); our findings isolate a more specific site in the network responsible for the core compositional operator underlying sentence comprehension.

We also discovered greater functional connectivity (via generalized phase-locking values for 3-50 Hz) between electrode pairs in pSTS-TOJ and both temporal pole and pars triangularis from 400-800ms after the presentation of the phrase-licensing nominal (Fig. 4). As noted, these structures are subserved by deep white matter pathways (Sarubbo et al., 2020). In relation to current findings and frameworks reviewed above, it is possible that the formation of phrase structure in pSTS-TOJ feeds categorial information (e.g. phrase type) to interpretation interfaces in ATL and memory/control interfaces in pars triangularis (a form of “spell-out”). One such piece of information encoded via PLV would be the phrase’s category/label (Murphy, 2015; Murphy and Shim, 2020). These results may point to a degree of top-down control from pars triangularis on initial phrase construction in pSTS-TOJ (Hagoort et al., 2009), however our current results cannot directly speak to this claim. These regions seem to be implicated in the retrieval and hierarchical composition of phrase structures, but the more precise computational role of such connectivity metrics requires further empirical, and conceptual, advances.

Generalizability to combinatoriality

Recent accounts in theoretical syntax consider the combinatorial process which binds morphemes into lexical items to be potentially analogous to the phrase-structure building operation Unification or Merge (required for any hierarchical compositional process), since morphemes also exhibit hierarchical relations between elements (Jackendoff and Audring, 2020; Rizzi, 2016). Inhibition of a portion of left posterior temporal lobe (pSTS, pSTG and temporo-parietal junction) selectively impairs the ability to produce appropriate functional morphemes, but does not effect any other sub-linguistic process such as semantic or lexical retrieval (Lee et al., 2018). Our data are compatible with the idea that in connection with other areas, such as IFG (Baggio and Hagoort, 2011; Zaccarella et al., 2021), pSTS-TOJ contributes to both morphological and phrasal unification (effectively the same computational operation, an instance of Merge). Our results also appear closely in line with a recent fMRI study exposing

a division between sensitivity to non-local dependency structure (in left anterior temporal pole and IFG) and sensitivity to phrase structure (in left pSTG) (Lopopolo et al., 2021). Another recent innovative paradigm in MEG, which kept conceptual structure uniform across conditions, pointed to the involvement of broad portions of posterior temporal cortex in computing syntactic complexity (Matar et al., 2021), while we have isolated a more specific portion in meaningful phrase composition.

While we did not find composition effects in inferior parietal lobule (in particular, angular gyrus), and had good electrode coverage here, this may be due to this region's role in higher-order semantic processing (e.g. thematic role assignment, discourse structure) and event structure (Boylan et al., 2015), rather than specifically minimal compositional schemes. For instance, there is a range of evidence that taxonomic conceptual relationships are encoded in ATL (in line with our findings), while thematic relationships are encoded in angular gyrus (Davis and Yee, 2019). Other evidence from intracranial recordings, examining alpha and theta suppression, reinforces this computational distinction between taxonomic and feature-based relations being encoded in ATL, and thematic/event-based relations being encoded in the inferior parietal lobule (IPL) (Thye et al., 2021). Morever, this particular intracranial study found clear low frequency effects in ATL and IPL in the complete absence of any broadband gamma differences.

Given the nature of our stimuli, we can make direct claims about semantic composition, since our composition/non-composition contrast was anchored around the word/pseudoword constrast. Nevertheless, in order to make more explicit claims about strictly syntactic compostion we will need to deploy a stimulus set contrasting some aspect of grammaticality within a minimal phrase paradigm. We therefore cannot currently make strong claims about minimal syntactic computations. We suspect, though, that portions of pSTS-TOJ are also implicated in minimal syntax, however the dynamics of the syntax network may differ from that of the semantic compositional network. Future work should explore such avenues as cross-frequency coupling (e.g. phase-amplitude, phase-phase) and Granger causality in order to build a comprehensive picture of the neural dynamics of phrasal comprehension.

Lexicality

Considering previous intracranial investigations of lexicality, pseudowords have induced greater high gamma activity than real words in left ventral temporal lobe (Tanji, 2005). Auditory recordings of verbs and pseudowords leads to gamma tracking of word processing with greater spatiotemporal specificity than any other frequency band (Canolty et al., 2007). This effect was localized to posterior and middle superior temporal gyrus (p/mSTG) and pSTS,

437 which our results appear to replicate (Humphries et al., 2006). In addition, we show recruitment
438 of anterior IFG in this process.

439 Lastly, our findings concerning ITC indicate that pSTG alpha may index the coordination of
440 smaller-scale ensembles which activate sub-lexical feature bundling to yield a coherent word-
441 level interpretation in auditory stimuli. The data structures implicated in this process appear to
442 include semantic features given that we found greater alpha ITC for words than for
443 pseudowords.

444 *Anticipatory response*

445 According to a range of parsing models (Berwick et al., 2019), adjective-noun syntax is
446 constructed predictively, in anticipation of the noun. Neural response differences in the period
447 preceding the noun in combinatorial trials would likely reflect the generation of this syntactic
448 structure. For instance, particular anticipatory amplitude increases have been isolated to the
449 alpha (8-12Hz) and beta (15-30Hz) bands in fronto-central scalp EEG electrodes and have
450 been related to the pre-activation of linguistic structure/information (Gastaldon et al., 2020;
451 Segaert et al., 2018), but a more precise localization is needed. Our documented anticipatory
452 effects in beta permit us to localise effects noted elsewhere (Bastiaansen and Hagoort, 2015;
453 Segaert et al., 2018). Beta oscillations in pars triangularis and ATL may be preparing a
454 syntactic slot to be filled by predicted upcoming nominal content, or they could be initiating
455 top-down local coordination of subsequent composition-indexing BGA in pSTS-TOJ. Following
456 other recent findings (Terporten et al., 2019), it is possible that these beta dynamics do not
457 pertain to lexico-semantic prediction specifically, but rather anticipatory stages pertaining to
458 phrasal initiation. Our findings are also potentially in line with the notion that beta oscillations
459 can index the construction and maintenance of sentence-level meaning (scaling up from
460 minimal phrases) (Lewis et al., 2016), and also the claims that beta can index aspects of
461 syntactic anticipation and phrasal category generation (Benítez-Burraco and Murphy, 2019;
462 Murphy, 2020), since all phrases were predictably nominal phrases.

463 We also discovered anticipatory effects in alpha in ATL, with a clear anterior-posterior
464 temporal distinction between power increases for anticipation (anterior) and decreases for no
465 anticipation (posterior). This posterior effect may relate strictly to lexical anticipation, since
466 non-anticipatory trials were always followed by a real noun; this alpha suppression may relate
467 to increased recruitment (Bonnefond & Jensen, 2013) of pSTS in late stage (pseudo-)lexical
468 processing effort (-200-0ms before the noun). The portion of temporal pole and MTG exhibiting
469 alpha increases during the anticipatory window could be also involved in late-stage lexico-
470 conceptual processing of adjectival representations, although given the relatively late post-
471 adjective window it is more likely to be related to anticipation. Relatedly, given increasing

evidence for IFG involvement in linear morpho-syntactic processing and complex sentential syntax (Matchin and Hickok, 2020), as opposed to elementary syntactic structure building, it is also possible that the beta effect in pars triangularis indexes a form of lexical anticipation (for word frequency effects in pars triangularis via functional coupling with subcentral gyrus, see Conner et al. 2019), with strictly syntactic anticipation being localized to temporal pole and MTG. A recent review of event-related potentials implicated in processing predictable words (the N400) also specifically pinpointed anterior IFG and LATL in preceding cortical activations (Pulvermüller and Grisoni, 2020), mapping onto the present results. Further, during basic semantic composition, anterior IFG has been shown to increase its activation level with the amount of lexical information being integrated into the structure (Schell et al., 2017), again pointing to a role for this region as a lexical memory buffer and locus of higher-order predictions.

Overall, summarizing the main effects and regions of interest, for phrase composition we discovered: greater BGA in pSTS-TOJ; greater low frequency (2-15 Hz) activity in temporal pole; greater functional connectivity between pSTS-TOJ and both temporal pole and pars triangularis. For phrase anticipation we discovered greater beta (15-30 Hz) activity in pars triangularis and temporal pole, and greater alpha (8-12 Hz) activity in temporal pole. For lexicality, we discovered greater BGA in widespread areas of IFG and posterior and superior temporal regions, and greater alpha ITC in pSTG. Lastly, for linguistic-visual unification we discovered greater BGA in IFS and anterior insula.

Materials and Methods

Participants: 18 patients (10 male, 18-41 years, IQ 95 ± 15, 2 left-handed) participated in the experiment after written informed consent was obtained. All were native English speakers. All experimental procedures were reviewed and approved by the Committee for the Protection of Human Subjects (CPHS) of the University of Texas Health Science Center at Houston as Protocol Number HSC-MS-06-0385.

Electrode Implantation and Data Recording: Data were acquired from either subdural grid electrodes (SDEs; 6 patients) or stereotactically placed depth electrodes (sEEGs; 12 patients) (Fig. 1B). SDEs were subdural platinum-iridium electrodes embedded in a silicone elastomer sheet (PMT Corporation; top-hat design; 3mm diameter cortical contact), and were surgically implanted via a craniotomy (Conner et al., 2011; Pieters et al., 2013; Tandon, 2012; Tong et al., 2020). sEEGs were implanted using a Robotic Surgical Assistant (ROSA; Medtech, Montpellier, France) (Rollo et al., 2020; Tandon et al., 2019). Each sEEG probe (PMT corporation, Chanhassen, Minnesota) was 0.8 mm in diameter and had 8-16 electrode

contacts. Each contact was a platinum-iridium cylinder, 2.0 mm in length and separated from the adjacent contact by 1.5-2.43 mm. Each patient had 12-20 such probes implanted. Following surgical implantation, electrodes were localized by co-registration of pre-operative anatomical 3T MRI and post-operative CT scans in AFNI (Cox, 1996). Electrode positions were projected onto a cortical surface model generated in FreeSurfer (Dale et al., 1999), and displayed on the cortical surface model for visualization (Pieters et al., 2013). Intracranial data were collected during research experiments starting on the first day after electrode implantation for sEEGs and two days after implantation for SDEs. Data were digitized at 2 kHz using the NeuroPort recording system (Blackrock Microsystems, Salt Lake City, Utah), imported into Matlab, initially referenced to the white matter channel used as a reference for the clinical acquisition system and visually inspected for line noise, artifacts and epileptic activity. Electrodes with excessive line noise or localized to sites of seizure onset were excluded. Each electrode was re-referenced to the common average of the remaining channels. Trials contaminated by inter-ictal epileptic spikes and trials in which participants responded incorrectly were discarded.

Stimuli and Experimental Design: Participants were presented with two-word auditory phrases, grouped by three conditions: Adjective-Noun ("red boat"), Adjective-Pseudoword ("red neub"), Pseudoword-Noun ("zuik boat"). To ensure attention was maintained, after each trial, participants were shown a colored drawing and asked to press a button indicating whether the picture matched the phrase they had just heard. Participants were told to respond positively only when the picture fully matched the phrase (e.g. the phrase "red boat" followed by a picture of a red car, or a blue boat, would be negative).

A fixation cross was presented in the centre of the screen for 700ms followed by the first word and 800ms later the second word was presented. 1600ms after the onset of the second word the picture was presented, and 1400ms after picture presentation participants were prompted to respond (Fig. 1A). Following their response, a blank screen was shown for 1500ms. Stimuli were presented in a pseudorandom order, with no repetition amongst items. The number of trials per block across the full experiment was as follows: Adjective-Noun (80), Pseudoword-Noun (40), Adjective-Pseudoword (40). All patients undertook 2 blocks. Half of the Adjective-Noun trials matched the picture presented (i.e. "red boat" was heard by the patient, and a picture of a red boat was then presented), and the other half did not match. 6 adjectives were used: black, blue, brown, green, pink, red (length M: 4.3, SD: 0.7; SUBTLEXus log-frequency 3.64). 20 nouns were used: bag, bell, boat, bone, cane, cross, cup, disc, flag, fork, hand, heart, house, key, lamp, leaf, lock, plane, shoe, star (length M: 4.0, SD: 0.6; log-frequency 3.38) (Brysbaert et al., 2012). 6 pseudowords were used: beeg, cresp, kleg, nar, neub, zuik (length

M: 4.0, SD: 0.6). Average stimuli length: Adjectives (420 ms), Nouns (450 ms), Pseudowords (430ms).

Stimuli were presented using Psychtoolbox (Kleiner et al., 2007) on a 15.4" LCD screen positioned at eye-level, 2-3' from the patient. Auditory stimuli were presented using stereo speakers (44.1 kHz, MacBook Pro 2008).

Signal Analysis: A total of 3250 electrode contacts were implanted in these patients; 2303 of these were included for analysis after excluding channels proximal to the seizure onset zone or exhibiting excessive inter-ictal spikes or line noise. Analyses were performed by first bandpass filtering the raw data of each electrode into broadband gamma activity (BGA; 70-150 Hz) following removal of line noise and its harmonics (zero-phase 2nd order Butterworth band-stop filters). Electrodes were also visually inspected for saccade artefacts. A frequency domain bandpass Hilbert transform (paired sigmoid flanks with half-width 1.5 Hz) was applied and the analytic amplitude was smoothed (Savitzky-Golay FIR, 3rd order, frame length of 251ms; Matlab 2019b, Mathworks, Natick, MA). BGA was defined as percentage change from baseline level; -500 to -100ms before the presentation of the first word in each trial. Periods of significant activation were tested using a one-tailed t-test at each time point and were corrected for multiple comparisons with a Benjamini-Hochberg false detection rate (FDR) threshold of $q<0.05$. For the grouped analysis, all electrodes were averaged within each subject and then the between-subject averages were used.

To provide statistically robust and topologically precise estimates of BGA, and to account for variations in sampling density, population-level representations were created using surface-based mixed-effects multilevel analysis (SB-MEMA) (Conner et al., 2011; Fischl et al., 1999; Kadipasaoglu et al., 2014, 2015). This method accounts for sparse sampling, outlier inferences, as well as intra- and inter-subject variability to produce population maps of cortical activity. A geodesic Gaussian smoothing filter (3 mm full-width at half-maximum) was applied. Significance levels were computed at a corrected alpha-level of 0.01 using family-wise error rate corrections for multiple comparisons. The minimum criterion for the family-wise error rate was determined by white-noise clustering analysis (Monte Carlo simulations, 5000 iterations) of data with the same dimension and smoothness as that analyzed (Kadipasaoglu et al., 2014). Results were further restricted to regions with at least three patients contributing to coverage and BGA percent change exceeding 5%.

Anatomical groups of electrodes were delineated, firstly, through indexing electrodes to the closest node on the standardized cortical surface (Saad and Reynolds, 2012), and secondly, through grouping channels into parcellations determined by Human Connectome Project (HCP) space (Glasser et al., 2016). Parametric statistics were used since HCP regions of

interest contained >30 electrodes. When contrasting experimental conditions, two-sided paired t-tests were evaluated at each time point for each region and significance levels were computed at $q<0.01$ using an FDR correction for multiple comparisons.

To generate event-related potentials (ERPs), the raw data were band pass filtered (0.1–50 Hz). Trials were averaged together and the resultant waveform was smoothed (Savitzky-Golay FIR, third-order, frame length of 251 ms). To account for differences in polarity between electrodes, ERPs were converted to root mean square (RMS), using a 50 ms sliding window. All electrodes were averaged within each subject, within ROI, and then the between subject averages were used.

There is increasing evidence that the phase of activation across distributed neural populations correlates with distinct underlying neural processes from the amplitude (Buzsáki, 2019; Fries, 2015; Sauseng and Klimesch, 2008). We therefore also investigated the influence of lexicality and phrase construction on inter-trial phase coherence (ITC). Phase information was extracted from the band-pass filtered data (8 – 12 Hz; zero-phase 3rd order Butterworth band-pass filter) using a Hilbert transform. ITC was calculated as the circular mean (absolute vector length) of instantaneous phase of stimulus-aligned trials computed as the median value of 10 iterations of a random 50% of trials.

To explore the functional connectivity between regions of interest during phrase composition, we used a generalized phase-locking analysis to estimate the dominant spatio-temporal distributions of field activity, and the strength of the coupling between them. Phase information was extracted from the down-sampled (200 Hz) and wide band-pass filtered data (3 – 50 Hz; zero-phase 8th order Butterworth band-pass filter) using the 'generalized phase' method (Davis et al., 2020) with a single-sided Fourier transform approach (Marple, 1999). This method captures the phase of the predominant fluctuations in the wideband signal and minimizes filter-related distortion of the waveform. PLV was calculated as the circular mean (absolute vector length) of the instantaneous phase difference between each electrode pair at each time point and baselined to the period −500 to −100 ms before onset of the first word. Statistics were calculated using the mean PLV of correctly answered trials between 0 to 500 ms after second word onset, comparing against a null distribution generated by randomly re-pairing trial recordings across the electrode pairs 500 times. Significant PLV was accepted at a threshold of $p<0.05$.

611 **Acknowledgements**

612 We express our gratitude to all the patients who participated in this study; the neurologists at
613 the Texas Comprehensive Epilepsy Program who participated in the care of these patients;
614 and the nurses and technicians in the Epilepsy Monitoring Unit at Memorial Hermann Hospital
615 who helped make this research possible. This work was supported by the National Institute of
616 Neurological Disorders and Stroke NS098981. Human subjects: Patients participated in the
617 experiments after written informed consent was obtained. All experimental procedures were
618 reviewed and approved by the Committee for the Protection of Human Subjects (CPHS) of
619 the University of Texas Health Science Center at Houston as Protocol Number: HSC-MS-06-
620 0385.

References

Antonucci, S., Beeson, P., Labiner, D., and Rapcsak, S. (2008). Lexical retrieval and semantic knowledge in patients with left inferior temporal lobe lesions. Aphasiology *22*, 281–304.

Arya, R. (2019). Similarity of spatiotemporal dynamics of language-related ECoG high-gamma modulation in Japanese and English speakers. Clin. Neurophysiol. *130*, 1403–1404.

Baggio, G., and Hagoort, P. (2011). The balance between memory and unification in semantics: A dynamic account of the N400. Lang. Cogn. Process. *26*, 1338–1367.

Bastiaansen, M., and Hagoort, P. (2015). Frequency-based Segregation of Syntactic and Semantic Unification during Online Sentence Level Language Comprehension. J. Cogn. Neurosci. *27*, 2095–2107.

Bemis, D.K., and Pylkkänen, L. (2011). Simple composition: A magnetoencephalography investigation into the comprehension of minimal linguistic phrases. J. Neurosci. *31*, 2801–2814.

Bemis, D.K., and Pylkkänen, L. (2013). Combination across domains: An MEG investigation into the relationship between mathematical, pictorial, and linguistic processing. Front. Psychol. *3*, 583.

Benítez-Burraco, A., and Murphy, E. (2019). Why Brain Oscillations Are Improving Our Understanding of Language. Front. Behav. Neurosci.

Berwick, R.C., Stabler, E.P., Berwick, R.C., and Stabler, E.P. (2019). Minimalist parsing (Oxford: Oxford University Press).

Boylan, C., Trueswell, J.C., and Thompson-Schill, S.L. (2015). Compositionality and the angular gyrus: A multi-voxel similarity analysis of the semantic composition of nouns and verbs. Neuropsychologia *78*, 130–141.

Bozic, M., Fonteneau, E., Su, L., and Marslen-Wilson, W.D. (2015). Grammatical analysis as a distributed neurobiological function. Hum. Brain Mapp. *36*, 1190–1201.

Brennan, J., and Pylkkänen, L. (2012). The time-course and spatial distribution of brain activity associated with sentence processing. Neuroimage *60*, 1139–1148.

Brennan, J.R., Stabler, E.P., Van Wagenen, S.E., Luh, W.M., and Hale, J.T. (2016). Abstract linguistic structure correlates with temporal activity during naturalistic comprehension. Brain Lang. *157–158*, 81–94.

Brysbaert, M., New, B., and Keuleers, E. (2012). Adding part-of-speech information to the SUBTLEX-US word frequencies. Behav. Res. Methods *44*, 991–997.

Buzsáki, G. (2019). The Brain from Inside Out (Oxford: Oxford University Press).

Buzsáki, G., and Watson, B.O. (2012). Brain rhythms and neural syntax: implications for efficient coding of cognitive content and neuropsychiatric disease. Dialogues Clin. Neurosci. *14*, 345–367.

Canolty, R.T., Soltani, M., Dalal, S.S., Edwards, E., Dronkers, N.F., Nagarajan, S.S., Kirsch, H.E., Barbaro, N.M., and Knight, R.T. (2007). Spatiotemporal Dynamics of Word Processing in the Human Brain. Front. Neurosci. *1*, 185–196.

Cazzoli, D., Kaufmann, B.C., Paladini, R.E., Müri, R.M., Nef, T., and Nyffeler, T. (2021). Anterior insula and inferior frontal gyrus: where ventral and dorsal visual attention systems meet. Brain Commun.

Chomsky, N. (1995). The Minimalist Program (Cambridge, MA: MIT Press).

Chomsky, N., Gallego, A.J., and Ott, D. (2019). Generative grammar and the faculty of language: insights, questions, and challenges. Catalan J. Linguist. Spec. Issue 226–261.

Conner, C.R., Ellmore, T.M., Pieters, T.A., di Sano, M.A., and Tandon, N. (2011). Variability of the relationship between electrophysiology and BOLD-fMRI across cortical regions in humans. J. Neurosci. *31*, 12855–12865.

Conner, C.R., Kadipasaoglu, C.M., Shouval, H.Z., Hickok, G., and Tandon, N. (2019). Network dynamics of Broca's area during word selection. PLoS One *14*, 1–30.

Cox, R.W. (1996). AFNI: Software for Analysis and Visualization of Functional Magnetic Resonance Neuroimages. Comput. Biomed. Res. *29*, 162–173.

Dale, A.M., Fischl, B., and Sereno, M.I. (1999). Cortical Surface-Based Analysis: I. Segmentation and Surface Reconstruction. Neuroimage *9*, 179–194.

Davis, C.P., and Yee, E. (2019). Features, labels, space, and time: factors supporting taxonomic relationships in the anterior temporal lobe and thematic relationships in the angular gyrus. Lang. Cogn. Neurosci. *34*, 1347–1357.

Davis, Z.W., Muller, L., Martinez-Trujillo, J., Sejnowski, T., and Reynolds, J.H. (2020). Spontaneous travelling cortical waves gate perception in behaving primates. Nature *587*, 432–436.

Duffau, H., Moritz-Gasser, S., and Mandonnet, E. (2014). A re-examination of neural basis of language processing: Proposal of a dynamic hodotopical model from data provided by brain stimulation mapping during picture naming. Brain Lang. *131*, 1–10.

Fedorenko, E., Scott, T.L., Brunner, P., Coon, W.G., Pritchett, B., Schalk, G., and Kanwisher, N. (2016). Neural correlate of the construction of sentence meaning. Proc. Natl. Acad. Sci. U. S. A. *113*, E6256–E6262.

Feng, X., Altarelli, I., Monzalvo, K., Ding, GuoshengRamus, F., Shu, H., Dehaene, S., Meng, X., and Dehaene-Lambertz, G. (2020). A universal reading network and its modulation by writing system and reading ability in

French and Chinese children. Elife *9*, e54591.

Figley, T.D., Mortazavi Moghadam, B., Bhullar, N., Kornelsen, J., Courtney, S.M., and Figley, C.R. (2017). Probabilistic white matter atlases of human auditory, basal ganglia, language, precuneus, sensorimotor, visual and visuospatial networks. Front. Hum. Neurosci. *11*, 1–12.

Fischl, B., Sereno, M.I., and Dale, A.M. (1999). Cortical surface-based analysis: II. Inflation, flattening, and a surface-based coordinate system. Neuroimage *9*, 195–207.

Flick, G., and Pylkkänen, L. (2020). Isolating syntax in natural language: MEG evidence for an early contribution of left posterior temporal cortex. Cortex *127*, 42–57.

Flick, G., Oseki, Y., Kaczmarek, A.R., Al Kaabi, M., Marantz, A., and Pylkkänen, L. (2018). Building words and phrases in the left temporal lobe. Cortex *106*, 213–236.

Flinker, A., Chang, E.F., Barbaro, N.M., Berger, M.S., and Knight, R.T. (2011). Sub-centimeter language organization in the human temporal lobe. Brain Lang. *117*, 103–109.

Fries, P. (2015). Rhythms for Cognition: Communication through Coherence. Neuron *88*, 220–235.

Gastaldon, S., Arcara, G., Navarrete, E., and Peressotti, F. (2020). Commonalities in alpha and beta neural desynchronizations during prediction in language comprehension and production. Cortex *133*, 328–345.

Glasser, M.F., Coalson, T.S., Robinson, E.C., Hacker, C.D., Harwell, J., Yacoub, E., Ugurbil, K., Andersson, J., Beckmann, C.F., Jenkinson, M., et al. (2016). A multi-modal parcellation of human cerebral cortex. Nature *536*, 171–178.

Graessner, A., Zaccarella, E., and Hartwigsen, G. (2021). Differential contributions of left-hemispheric language regions to basic semantic composition. Brain Struct. Funct.

Hagoort, P. (2003). How the brain solves the binding problem for language: A neurocomputational model of syntactic processing. Neuroimage *20*, S18–S29.

Hagoort, P. (2004). Integration of Word Meaning and World Knowledge in Language Comprehension. Science (80-.). *304*, 438–441.

Hagoort, P. (2005). On Broca, brain, and binding: A new framework. Trends Cogn. Sci.

Hagoort, P. (2013). MUC (Memory, Unification, Control) and beyond. Front. Psychol. *4*.

Hagoort, P. (2017). The core and beyond in the language-ready brain. Neurosci. Biobehav. Rev. *81*, 194–204.

Hagoort, P. (2020). The meaning-making mechanism(s) behind the eyes and between the ears. Philos. Trans. R.

Soc. Lond. B. Biol. Sci. *375*, 20190301.

Hagoort, P., and Indefrey, P. (2014). The Neurobiology of Language Beyond Single Words. Annu. Rev. Neurosci. *37*, 347–362.

Hagoort, P., Baggio, G., and Willems, R.M. (2009). Semantic unification. In The Cognitive Neurosciences, M.S. Gazzaniga, ed. (MIT Press), pp. 819–836.

Hovsepyan, S., Olasagasti, I., and Giraud, A.-L. (2020). Combining predictive coding and neural oscillations enables online syllable recognition in natural speech. Nat. Commun. *11*, 3117.

Humphries, C., Binder, J.R., Medler, D.A., and Liebenthal, E. (2006). Syntactic and semantic modulation of neural activity during auditory sentence comprehension. J. Cogn. Neurosci. *18*, 665–679.

Irimia, A., Van Horn, J.D., and Halgren, E. (2012). Source cancellation profiles of electroencephalography and magnetoencephalography. Neuroimage *59*, 2464–2474.

Jackendoff, R., and Audring, J. (2020). The Texture of the Lexicon: Relational Morphology and the Parallel Architecture (Oxford: Oxford University Press).

Jensen, O., Spaak, E., and Zumer, J.M. (2019). Human brain oscillations: From physiological mechanisms to analysis and cognition. In Magnetoencephalography: From Signals to Dynamic Cortical Networks: Second Edition, p.

Kadipasaoglu, C.M., Baboyan, V.G., Conner, C.R., Chen, G., Saad, Z.S., and Tandon, N. (2014). Surface-based mixed effects multilevel analysis of grouped human electrocorticography. Neuroimage *101*, 215–224.

Kadipasaoglu, C.M., Forseth, K., Whaley, M., Conner, C.R., Rollo, M.J., Baboyan, V.G., and Tandon, N. (2015). Development of grouped icEEG for the study of cognitive processing. Front. Psychol. *6*.

Kleiner, M., Brainard, D., Pelli, D., Ingling, A., Murray, R., and Broussard, C. (2007). What's new in psychtoolbox-3. Perception *36*, 1–16.

Kucyi, A., and Parvizi, J. (2020). Pupillary Dynamics Link Spontaneous and Task-Evoked Activations Recorded Directly from Human Insula. J. Neurosci. *40*, 6207–6218.

Lambon Ralph, M.A., Ehsan, S., Baker, G.A., and Rogers, T.T. (2012). Semantic memory is impaired in patients with unilateral anterior temporal lobe resection for temporal lobe epilepsy. Brain *135*, 242–258.

Lau, E., Stroud, C., Plesch, S., and Phillips, C. (2006). The role of structural prediction in rapid syntactic analysis. Brain Lang. *98*, 74–88.

Law, R., and Pylkkänen, L. (2021). Lists with and without Syntax: A New Approach to Measuring the Neural Processing of Syntax. J. Neurosci. *41*, 2186–2196.

Lee, D.K., Fedorenko, E., Simon, M. V., Curry, W.T., Nahed, B. V., Cahill, D.P., and Williams, Z.M. (2018). Neural encoding and production of functional morphemes in the posterior temporal lobe. Nat. Commun. *9*, 1877.

Lewis, A.G., Schoffelen, J.M., Schriefers, H., and Bastlaansen, M. (2016). A predictive coding perspective on beta oscillations during sentence-level language comprehension. Front. Hum. Neurosci. *10*, 83.

Lopopolo, A., van den Bosch, A., Petersson, K.-M., and Willems, R.M. (2021). Distinguishing Syntactic Operations in the Brain: Dependency and Phrase-Structure Parsing. Neurobiol. Lang. *2*, 152–175.

Marko, M., Cimrová, B., and Riečanský, I. (2019). Neural theta oscillations support semantic memory retrieval. Sci. Rep. *9*, 17667.

Marple, L. (1999). Computing the discrete-time “analytic” signal via FFT. IEEE Trans. Signal Process. *47*, 2600–2603.

Martin, S., Millán, J. del R., Knight, R.T., and Pasley, B.N. (2019). The use of intracranial recordings to decode human language: Challenges and opportunities. Brain Lang. *193*, 73–83.

Matar, S., Dirani, J., Marantz, A., and Pylkkänen, L. (2021). Left posterior temporal cortex is sensitive to syntax within conceptually matched Arabic expressions. Sci. Rep. *11*.

Matchin, W., and Hickok, G. (2020). The Cortical Organization of Syntax. Cereb. Cortex *30*, 1481–1498.

Muller, L., Chavane, F., Reynolds, J., and Sejnowski, T.J. (2018). Cortical travelling waves: mechanisms and computational principles. Nat. Rev. Neurosci. *19*, 255–268.

Murphy, E. (2015). Labels, cognomes, and cyclic computation: An ethological perspective. Front. Psychol. *6*.

Murphy, E. (2018). Interfaces (travelling oscillations) + recursion (delta-theta code) = language. In The Talking Species: Perspectives on the Evolutionary, Neuronal and Cultural Foundations of Language, E. Luef, and M. Manuela, eds. (Graz), pp. 251–269.

Murphy, E. (2020). The Oscillatory Nature of Language (Cambridge: Cambridge University Press).

Murphy, E., and Shim, J.-Y. (2020). Copy invisibility and (non-)categorial labeling. Linguist. Res. *37*, 187–215.

Nelson, M.J., El Karoui, I., Giber, K., Yang, X., Cohen, L., Koopman, H., Cash, S.S., Naccache, L., Hale, J.T., Pallier, C., et al. (2017). Neurophysiological dynamics of phrase-structure building during sentence processing. Proc. Natl. Acad. Sci. U. S. A. *114*, E3669–E3678.

762 Neufeld, C., Kramer, S.E., Lapinskaya, N., Heffner, C.C., Malko, A., and Lau, E.F. (2016). The electrophysiology
763 of basic phrase building. PLoS One *11*, 1–22.

764 Packard, P.A., Steiger, T.K., Fuentemilla, L., and Bunzeck, N. (2020). Neural oscillations and event-related
765 potentials reveal how semantic congruence drives long-term memory in both young and older humans. Sci. Rep.

766 Pieters, T.A., Conner, C.R., and Tandon, N. (2013). Recursive grid partitioning on a cortical surface model: an
767 optimized technique for the localization of implanted subdural electrodes. J. Neurosurg. *118*, 1086–1097.

768 Pietroski, P.M. (2018). Conjoining meanings: Semantics without truth values (Oxford: Oxford University Press).

769 Pobric, G., Jefferies, E., and Lambon Ralph, M.A. (2010). Category-Specific versus Category-General Semantic
770 Impairment Induced by Transcranial Magnetic Stimulation. Curr. Biol. *20*, 964–968.

771 Prystauka, Y., and Lewis, A.G. (2019). The power of neural oscillations to inform sentence comprehension: A
772 linguistic perspective. Lang. Linguist. Compass *13*.

773 Pulvermüller, F., and Grisoni, L. (2020). Semantic prediction in brain and mind. Trends Cogn. Sci. *24*, 781–784.

774 Pylkkänen, L. (2020). Neural basis of basic composition: what we have learned from the red-boat studies and
775 their extensions. Philos. Trans. R. Soc. Lond. B. Biol. Sci. *375*, 20190299.

776 Pylkkänen, L., and Brennan, J. (2020). Composition: the neurobiology of syntactic and semantic phrase structure
777 building. In The Cognitive Neurosciences, D. Poeppel, G.. Mangun, and M.. Gazzaniga, eds. (Cambridge, MA:
778 MIT Press), p.

779 Rizzi, L. (2016). Monkey morpho-syntax and merge-based systems. Theor. Linguist. *42*, 139–145.

780 Rollo, P.S., Rollo, M.J., Zhu, P., Woolnough, O., and Tandon, N. (2020). Oblique trajectory angles in robotic
781 stereo-electroencephalography. J. Neurosurg. 1–10.

782 Saad, Z.S., and Reynolds, R.C. (2012). SUMA. Neuroimage *62*, 768–773.

783 Safavi, S., Panagiotaropoulos, T., Kapoor, V., Ramirez-Villegas, J.F., Logothetis, N.K., and Besserve, M. (2020).
784 Uncovering the organization of neural circuits with generalized phase locking analysis. BioRxiv.

785 Sarubbo, S., Tate, M., De Benedictis, A., Merler, S., Moritz-Gasser, S., Herbet, G., and Duffau, H. (2020).
786 Mapping critical cortical hubs and white matter pathways by direct electrical stimulation: an original functional
787 atlas of the human brain. Neuroimage *205*, 116237.

788 Sauseng, P., and Klimesch, W. (2008). What does phase information of oscillatory brain activity tell us about
789 cognitive processes? Neurosci. Biobehav. Rev. *32*, 1001–1013.

Schell, M., Zaccarella, E., and Friederici, A.D. (2017). Differential cortical contribution of syntax and semantics: An fMRI study on two-word phrasal processing. Cortex *96*, 105–120.

Segaert, K., Mazaheri, A., and Hagoort, P. (2018). Binding language: structuring sentences through precisely timed oscillatory mechanisms. Eur. J. Neurosci. *48*, 2651–2662.

Tandon, N. (2012). Mapping of human language. In Clinical Brain Mapping, D. Yoshor, and E. Mizrahi, eds. (McGraw Hill Education), pp. 203–218.

Tandon, N., Tong, B.A., Friedman, E.R., Johnson, J.A., Von Allmen, G., Thomas, M.S., Hope, O.A., Kalamangalam, G.P., Slater, J.D., and Thompson, S.A. (2019). Analysis of Morbidity and Outcomes Associated with Use of Subdural Grids vs Stereoelectroencephalography in Patients with Intractable Epilepsy. JAMA Neurol. *76*, 672–681.

Tanji, K. (2005). High-Frequency -Band Activity in the Basal Temporal Cortex during Picture-Naming and Lexical-Decision Tasks. J. Neurosci. *25*, 3287–3293.

Terporten, R., Schoffelen, J.M., Dai, B., Hagoort, P., and Kösem, A. (2019). The Relation between Alpha/Beta Oscillations and the Encoding of Sentence induced Contextual Information. Sci. Rep. *9*, 1–12.

Thye, M., Geller, J., Szaflarski, J.P., and Mirman, D. (2021). Intracranial EEG evidence of functional specialization for taxonomic and thematic relations. Cortex.

Tong, B.A., Esquenazi, Y., Johnson, J., Zhu, P., and Tandon, N. (2020). The Brain is Not Flat: Conformal Electrode Arrays Diminish Complications of Subdural Electrode Implantation, A Series of 117 Cases. World Neurosurg. *144*, e734–e742.

Trettenbrein, P., Papitto, G., Friederici, A.D., and Zaccarella, E. (2020). Functional neuroanatomy of language without speech: An ALE meta-analysis of sign language. Hum. Brain Mapp. *doi.org/10*.

Vogelzang, M., Thiel, C.M., Rosemann, S., Rieger, J.W., and Ruigendijk, E. (2020). Neural Mechanisms Underlying the Processing of Complex Sentences: An fMRI Study. Neurobiol. Lang. *1*, 226–248.

Wang, X., Men, W., Gao, J., Caramazza, A., and Bi, Y. (2020). Two Forms of Knowledge Representations in the Human Brain. Neuron *107*, 383–393.

Westerlund, M., and Pylkkänen, L. (2014). The role of the left anterior temporal lobe in semantic composition vs. semantic memory. Neuropsychologia *57*, 59–70.

Westerlund, M., Kastner, I., Al Kaabi, M., and Pylkkänen, L. (2015). The LATL as locus of composition: MEG evidence from English and Arabic. Brain Lang. *141*, 124–134.

Wilson, S.M., and Saygin, A.P. (2004). Grammaticality Judgment in Aphasia: Deficits Are Not Specific to Syntactic Structures, Aphasic Syndromes, or Lesion Sites. J. Cogn. Neurosci. *16*, 238–252.

Wilson, S.M., DeMarco, A.T., Henry, M.L., Gesierich, B., Babiak, M., Mandelli, M.L., Miller, B.L., and Gorno-Tempini, M.L. (2014). What role does the anterior temporal lobe play in sentence-level processing? neural correlates of syntactic processing in semantic variant primary progressive aphasia. J. Cogn. Neurosci. *26*, 970–985.

Woolnough, O., Forseth, K.J., Rollo, P.S., and Tandon, N. (2019). Uncovering the functional anatomy of the human insula during speech. Elife *8*, 1–14.

Zaccarella, E., Papitto, G., and Friederici, A.D. (2021). Language and action in Broca's area: Computational differentiation and cortical segregation. Brain Cogn. *147*, 105651.

Zhang, L., and Pylkkänen, L. (2018). Semantic composition of sentences word by word: MEG evidence for shared processing of conceptual and logical elements. Neuropsychologia *119*, 392–404.

Supplementary Figures

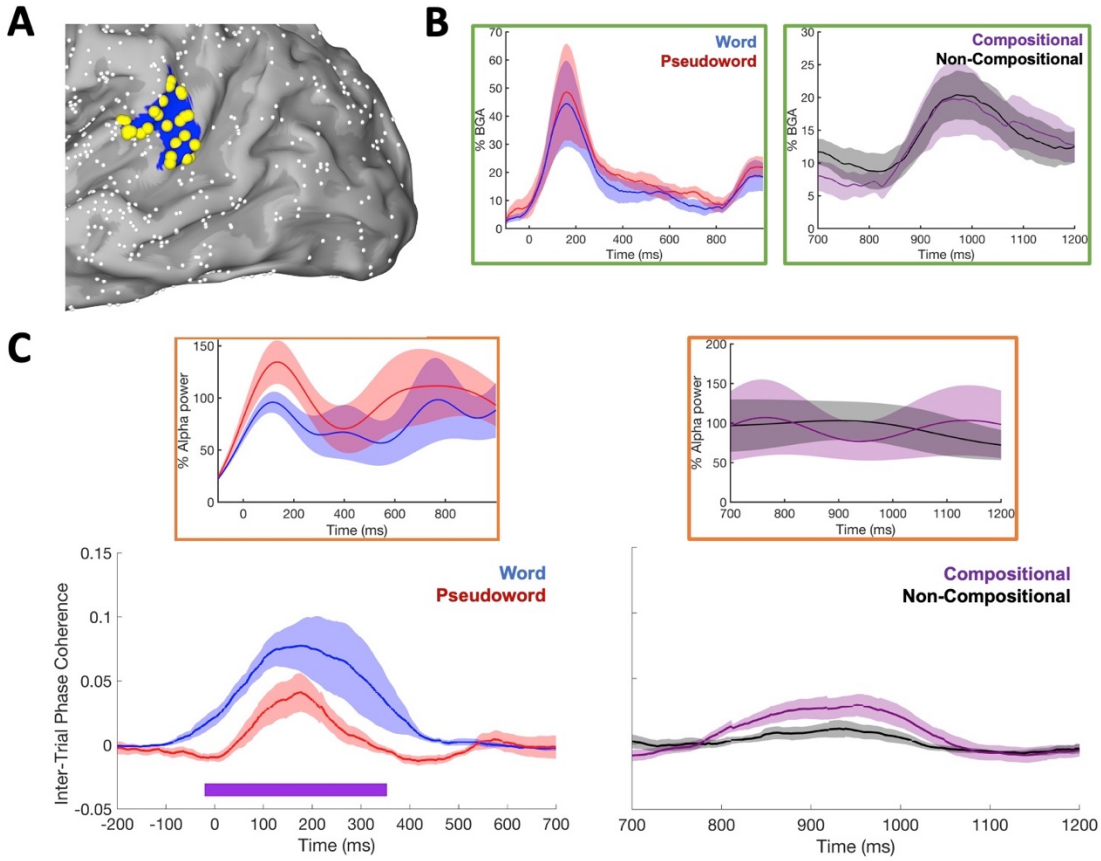

<u>Supplementary Figure 1</u>: Inter-trial phase coherence and lexicality.

(A) Electrodes with significant differences in ITC for words vs pseudowords, in a portion of posterior temporal cortex with a high concentration of electrodes exhibiting significant differences (9 patients); HCP index: area STV (Glasser et al., 2016). (B) Gamma traces (green dashed box) for electrodes in (A) for words vs. pseudowords and compositional vs. non-compositional trials (C) ITC in alpha (8-12Hz) for all electrodes in (A) for words (blue) and pseudowords (red) on the left, with alpha (orange dashed box) amplitude traces, and for phrase composition (purple) and non-composition (black) on the right isolated around the onset of the second word (no significant effect for composition contrast). T0 = first word onset.

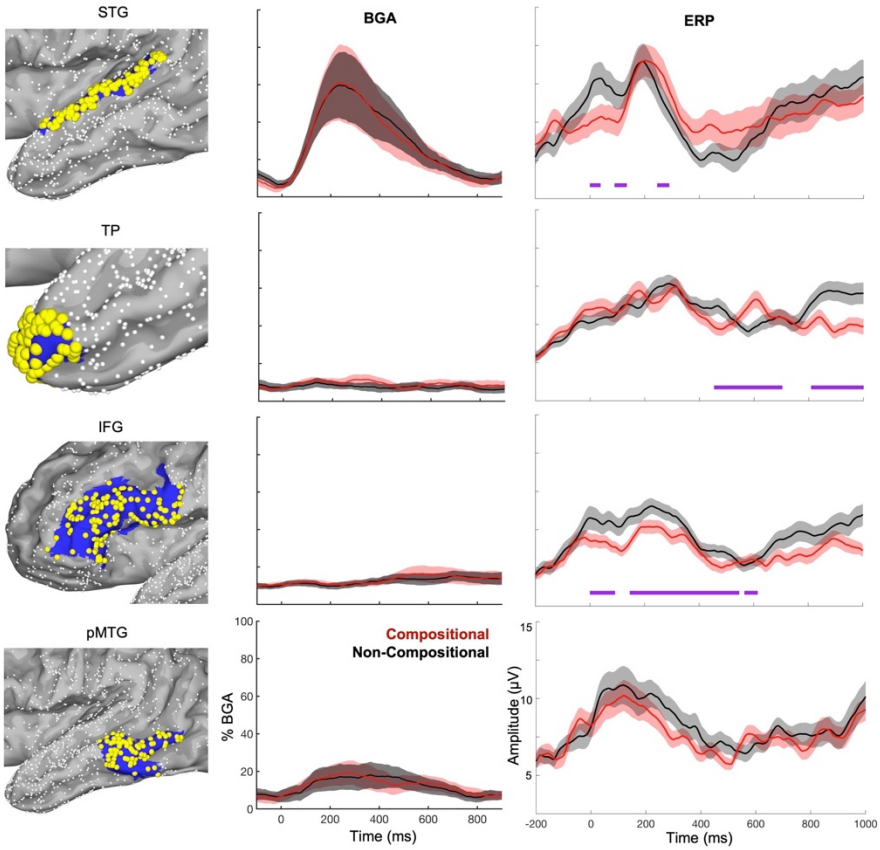

<u>Supplementary Figure 2</u>: Regions of interest and their BGA/ERP signatures. Regional broadband gamma amplitude (middle column) with event-related potentials (right column). Red: Compositional. Black: Non-Compositional. HCP index from top-down: posterior superior temporal gyrus (pSTG) = [A4]; temporal pole = [TGd]; inferior frontal gyrus (IFG) = [FOP4, 44, 45, IFSp, p47r, IFSa, 47l]; posterior middle temporal gyrus (pMTG) = [PHT, TE1p]. BGA traces are thresholded by $p<0.05$ significantly active from baseline (first word onset, -500 to -100ms) with a minimum of 10% BGA amplitude increase during the 100-400ms post-second word onset period. ERPs were computed across the four ROIs plotted on the left column, with significant condition differences being computed across 0-1000ms in the same (FDR-corrected) manner as the BGA plots (see Methods).